Modelling of Circadian Rhythms in *Drosophila* Incorporating the Interlocked PER/TIM and VRI/PDP1 Feedback Loops

Z. Xie, D. Kulasiri

Centre for Advanced Computational Solutions (C-fACS), Lincoln University, Canterbury, New Zealand

Abstract

Circadian rhythms of gene activity, metabolism, physiology and behaviour are observed in all the eukaryotes and some prokaryotes. In this study, we present a model to represent the transcriptional regulatory network essential for the circadian rhythmicity in *Drosophila*. The model incorporates the transcriptional feedback loops revealed so far in the network of the circadian clock (PER/TIM and VRI/PDP1 loops). Conventional Hill functions are not assumed to describe the regulation of genes, instead of the explicit reactions of binding and unbinding processes of transcription factors to promoters are modelled. The model simulates sustained circadian oscillations in mRNA and protein concentrations in constant darkness in agreement with experimental observations. It also simulates entrainment by light-dark cycles, disappearance of the rhythmicity in constant light and the shape of phase response curves resembling that of the experimental results. The model is robust over a wide range of parameter variations. In addition, the simulated E-box mutation, per^S and per^L mutants are similar to that observed in the experiments. The deficiency between the simulated mRNA levels and experimental observations in per^{01}, tim^{01} and clk^{Jrk} mutants suggests some difference on the part of the model from reality.

Keywords: Computational biology; Mathematical models; Circadian rhythms; Circadian clock; Oscillations

1. Introduction

All the eukaryotes and some prokaryotes are capable of maintaining sustained oscillations in terms of gene activity, metabolism, physiology and behaviour with circadian periods. These oscillations are known as circadian rhythms. Circadian rhythms affect all aspects of daily life and have long provided a unique point from which to address fundamental and wide-ranging questions of physiology and behaviour. Now it is experimentally established that self-sustaining circadian clocks controlling circadian rhythms regulate hundreds of genes and allow organisms to anticipate daily changes to environmental influences (Pittendrigh 1993; 2003). In recent decades, many components and molecular mechanisms comprising the circadian clocks have been uncovered, largely due to advances in molecular biology experiments (Dunlap 1999). The model organisms include unicellular eukaryotes, fungi, plants, invertebrates and mammals (Young and Kay 2001). Among them *Drosophila* is one of the most intensively researched organisms because it is well suited to large-scale mutant screening and, consequently, a number of genes that contribute to the timing mechanism have been identified (Van Gelder, Herzog et al. 2003).

Mathematical modelling is useful for providing a framework for integrating data and gaining insights into the static and dynamic behaviour of complex networks, especially in the case of genetic regulatory networks where, generally, multiple feedback loops exist. The models can provide coarse-grained prediction, identify gaps in our biological knowledge and, if well constructed, predict new behaviours that can be explored experimentally (Endy and Brent 2001; Kitano 2002). Given the fertile experimental data about the molecular components and mechanisms in *Drosophila*, the circadian clock provides an excellent example for modelling in the hope of understanding its genetic regulation systematically (Goldbeter 2002). It has been revealed that at least six transcription factors, namely Period (PER), Timeless (TIM), Vrille (VRI), Par domain protein 1ε (PDP1), Cycle (CYC) and Clock (CLK)[1], play critical roles in the regulatory network of the circadian clock in *Drosophila* (Hardin 2005).

[1] We follow the notation that protein names are written in upper case, genes and mRNAs are in lower case.

A range of mathematical models for the circadian clock in *Drosophila* has been proposed in the literature. These models can be categorised according to their structures: (1) Single negative feedback model, where PER represses its own gene expression (Goldbeter 1995) or where PER/TIM dimers inhibit gene expression of *per* and *tim* (Leloup and Goldbeter 1998; Tyson, Hong et al. 1999); (2) Two interlocking feedback loops model, where *per* and *tim* expressions are activated by CLK/CYC dimers and suppressed by PER/TIM dimers, and *clk* expression is repressed by CLK/CYC and de-repressed by PER/TIM (Smolen, Baxter et al. 2001; Ueda, Hirose et al. 2002); (3) Most recent models involving *clk* expression activated by PDP1 and suppressed by VRI (Smolen, Hardin et al. 2004; Ruoff, Christensen et al. 2005). In this paper, we develop a mathematical model of gene expression for the five key components in the circadian clock in *Drosophila*.

A common characteristic of the previous models is that activation and repression processes are described by Hill functions which imply switch-like behaviour of the transcriptional effects. With such transcriptional description, these models have produced sustained oscillations in appropriate parameter regimes. However, the models do not account for binding of transcription factors to promoters due to the description of transcriptional processes by Hill functions. A general model for the circadian clocks developed by Vilar (Vilar, Kueh et al. 2002) and a mammalian circadian model proposed by Forger (Forger and Peskin 2003) include explicit descriptions of the binding and unbinding processes of transcription factors to promoters. We propose that such description needs to be incorporated into the *Drosophila* clock model to explore transcriptional behaviour more explicitly.

The purpose of this paper is to develop a deterministic model with a set of differential equations incorporating the core components known to us so far in the regulatory network (*per*, *tim*, *vri*, *pdp1* and *clk* genes and their products) for simulating circadian rhythms of *Drosophila*, and to compare the behaviour of the model using the published

experimental data. The structure of the paper is as follows: the molecular basis of the circadian clock of *Drosophila* is reviewed in Section 2; the rationale and detailed development of the model are described in Section 3; the simulation results of the model are compared with the experimental results in Section 4. Finally, the main findings of the paper are discussed in Section 5.

2. Review of molecular basis of the *Drosophila* circadian clock

The circadian system consists of three parts: an input pathway that relays environmental signals and passes them to the circadian clock; the circadian clock that autonomously produces circadian oscillations of clock components, with or without external stimuli; and an output pathway that regulates rhythmic biochemical and physiological activities in the cell (Schoning and Staiger 2005).

In *Drosophila*, a number of genes have been identified that are necessary for circadian clock functions. These genes can be divided into three categories according to the molecular nature of their protein products (Hardin 2005). These proteins include (1), transcriptional activators: CLK, CYC and PDP1; (2), transcriptional repressors: PER, TIM and VRI; and (3) the proteins that alter protein stability and subcellular localisation: Doubletime (DBT), Shaggy (SGG), Slimb (SLMB) and casein kinase 2 (CK2) (Hardin 2005).

Transcriptional regulation underlying the circadian clock in *Drosophila* includes two interacting feedback loops, as shown in Figure 1 (Glossop, Lyons et al. 1999; Cyran, Buchsbaum et al. 2003; Hardin 2005). The first loop, named the PER/TIM loop, starts with activation of *per* and *tim* expression from mid day. Activation of *per* and *tim* transcription is mediated by two transcription factors, CLK and CYC. Experiments have shown that CLK and CYC form dimers that target CACGTG enhancers (called E-boxes) in the *per* and *tim* promoters (Allada, 1998). After initial activation of *per* and *tim* expression, there is a 4 h – 6 h delay between the peak concentrations of *per* and *tim* mRNAs and that of PER and TIM proteins (Zerr, Hall et al. 1990; Zeng, Qian et al.

1996). As a result, CLK/CYC can continue to activate transcription of *per* and *tim* genes, while PER and TIM proteins accumulate in the cytoplasm. PER and TIM also form PER/TIM dimers while accumulating. In the middle of the night PER/TIM dimers are transported into the nucleus. After entering the nucleus, they can bind to CLK/CYC dimers effectively inhibiting CLK/CYC binding ability to E-boxes without disrupting the dimeric structure of CLK/CYC (Lee, Bae et al. 1998). This inhibition lasts until PER and TIM proteins are degraded. Then the expressions of *per* and *tim* are reactivated by CLK/CYC dimers the following mid day.

(Figure 1)

The second loop, named the VRI/PDP1 loop, consists a VRI-mediated negative feedback loop and a PDP1-medicated positive feedback loop. This loop starts with activation of *vri* and *pdp1* transcription by CLK/CYC during the late day and early night. Like *per* and *tim* genes, E-boxes are also found in the promoters of the *vri* and *pdp1* genes and CLK/CYC dimers have been shown to activate *vri* and *pdp1* expression *in vitro* in an E-box-dependent manner (Cyran, Buchsbaum et al. 2003; Glossop, Houl et al. 2003). VRI accumulates first in phase with its mRNA then PDP1 accumulates during the mid to late evening. Both VRI and PDP1 belong to basic zipper transcription factors with highly conserved basic DNA binding domains, suggesting that they bind to the same set of target genes. Indeed *in vitro* experiments showed VRI binds VRI/PDP1 box (V/P box) in the *clk* regulatory elements to inhibit *clk* transcription and PDP1 can compete with VRI for binding to V/P box and activates *clk* transcription (Cyran, Buchsbaum et al. 2003). The effects from the initial VRI-dependent repression in the early night and the subsequent PDP1-dependent activation in the middle to late night determine the rhythmic expression of *clk*. However, the newly produced CLK at the end of night and early morning is inactive temporally due to high levels of PER/TIM dimers induced by the previous produced CLK. Once PER/TIM dimers are degraded, CLK/CYC reactivates gene expression of *per*, *tim*, *vri* and *pdp1* and starts a new cycle.

In addition to regulation at the transcriptional level, many clock components in *Drosophila* are also regulated post-transcriptionally and post-translationally. For example, Doubletime (DBT) destabilises PER. Casein Kinase 2 (CK2) destabilises PER and also affects its nuclear localisation. Shaggy (SGG) phosphorylates TIM to promote nuclear localisation of PER/TIM dimers. Slimb (SLMB) targets phosphorylated PER for degradation (Hardin 2005). These processes are important to provide time delays between mRNAs and proteins. For example, a 4 h – 6 h delay between accumulation of *per* mRNA in the cytoplasm and PER in the nucleus results from the initial destabilisation of PER by DBT dependent phosphorylation, and possibly also CK2 dependent phosphorylation, followed by the stabilisation of PER by dimerisation with TIM before the nuclear entry (Price, Blau et al. 1998).

3. Model description

In this section we give assumptions on which the model is based on, and then provide the complete set of differential equations (Eq. 1 – 19). To solve the equations numerically, the parameters (in Table 1) and initial conditions (in Table 2) are also specified.

3.1. Model assumptions

The model of the circadian clock is schematised in detail (Figure 2). This model relies on a number of assumptions, and the rationale of the assumptions is as follows:

(Figure 2)

1. We ignore the separate nuclear and cytoplasmic compartments in the model; instead we assume that all the reactions take place over a whole cell. Although eukaryotic species have compartments separated by nuclear membranes and transcription factors have to be located into the nucleus in order to affect gene expression, some prokaryotes,

which lack a nucleus or nuclear envelope, such as cyanobacteria, can also generate circadian rhythms. This demonstrates that it is possible for cells to maintain sustained circadian rhythms without compartmentalisation. A theoretical study by Kurosawa (Kurosawa, Mochizuki et al. 2002) also showed that a cell can generate a sustained oscillation in the absence of compartmentalisation with a single negative feedback model.

2. Translation, degradation and dissociation of complex are assumed to be first-order reactions, and association process of complex is assumed to be second-order reactions. This keeps the model simple and the number of parameters low. The study by Kurosawa on a single negative feedback oscillator showed that by introducing Michaelis-Menten (MM) type kinetics within the model, oscillations and their robustness may be enhanced (Kurosawa, Mochizuki et al. 2002). In fact in many of previous circadian clock models, MM kinetics have been used. However, there is no justification about whether MM kinetics are correct description for these processes as they have not been understood in detail yet. It will be shown later that simulated oscillations are even more robust for the parameter variations used in our model.

3. Phosphorylation of proteins is not considered. Although we are aware that phosphorylation is important for providing the time delay between mRNAs and proteins as reviewed above, the focus of the current study is on the transcriptional regulation, and we do not include phosphorylation of proteins at this stage for the sake of simplification.

4. Gene expression of *per*, *tim*, *vri* and *pdp1* is activated by binding of CLK/CYC dimers to E-boxes in their promoter regions. Analysis of the first 4 kb of sequence upstream of the start site of *pdp1* transcription revealed six E-boxes (Cyran, Buchsbaum et al. 2003). The *vri* promoter sequence was searched and four E-boxes were found (Blau and Young 1999). In the *tim* promoter, three functional E-boxes were discovered within about 150 bp short distance (McDonald and Rosbash 2001). In addition, two TER boxes (11-bp Tim E-box-like repeats) serving as additional binding sites for CLK/CYC dimers were also found in the *tim* promoter (McDonald and Rosbash 2001).

Therefore, we assume five binding sites, including E-boxes and E-box-like binding sites, in the *tim* promoter region. In mammals, five E-boxes were found in the *per1* promoter (Yamaguchi, Mitsui et al. 2000) and we assume the case is similar in our model for the *per* promoter.

5. We assume that CLK/CYC dimers independently bind to individual E-boxes in a promoter. In the functional analysis of E-boxes in the mouse *mPer1* promoter, the levels of *mPer1* transcriptional expression activated by CLK/BMAL1 were roughly proportional to the number of conserved E-boxes (Hida, Koike et al. 2000). The result suggests that there is no or negligible cooperative interaction in the E-box binding activities of CLK/BMAL1. Since no information is available about cooperativity in the E-box binding activities by CLK/CYC in *Drosophila*, we treat it as the case in the *mPer1* promoter. For the same reason, we also assume that if CLK/CYC is bound to just one E-box for a given gene, the transcription of that gene is activated and the effect of binding additional E-boxes on transcription activation is additive (Hida, Koike et al. 2000).

6. PER/TIM dimers are assumed not to bind to CLK/CYC dimers if the later are bound to promoters. In mammals, mCRY complexes bind to CLK/BMAL1 and repress transcription without removing CLK/BMAL1 from E-boxes (Etchegaray, Lee et al. 2003). However in *Drosophila*, PER/TIM has not been shown to bind CLK/CYC complexes which are bound to E-boxes. (Yu, Zheng et al. 2006).

7. *In vitro* experiments showed that the concentration of CYC is always constitutive, with high levels in the cells (Glossop, Lyons et al. 1999). Therefore, we assume that the concentration of CYC in the system is constant (100 nM is assumed) so that there is always enough CYC bound to CLK to form dimers.

8. We assume that there is only one copy of the *per*, *tim*, *vri*, *pdp1* and *clk* genes in the model, this corresponds to concentration of 3.185×10^{-3} nM for each gene. The calculation is carried out as follows: a radius of lateral neuron in *Drosophila* is about 5 –

6 μm (Ewer, Frisch et al. 1992), and 5 μm is taken in our model. The volume of the cell is $V = 4/3\ \pi\ r^3 = 5.23\times10^{-13}$L. Therefore, the number of molecules that corresponds to 1 nM is $1\ \text{nM} = (5.23\times10^{-13}\text{L})(10^{-9}\text{mole/L})(6\times10^{23}\text{molecules/mole}) \approx 314$ molecules.

9. Because concentrations of 'clock' mRNAs and proteins in the cell are not known and only relative concentration abundance were measured, we follow one of the previous theoretical models (Vilar, Kueh et al. 2002) and assume around 1000 protein molecules and 100 mRNA molecules in a cell, which correspond to roughly protein concentrations of 3 – 4 nM and mRNA concentrations of 0.3 – 0.4 nM.

3.2. Kinetic equations

The model schematised in Figure 2 is described by 19 differential equations outlined below. For clarity, we group these equations into four categories. For the better visualisation, we write some of the variable names and rate constants in mixed normal and subscript fonts in the equations, they are however all written in normal font in Table 1, 2 and 3. The name of mRNAs is written in lower case with a subscript 'm' denoting mRNA. The name of proteins and complexes is written in upper case. Abbreviations used for variable names are: PDP for PDP1, CC for CLK/CYC dimer, PT for PER/TIM dimer and CCPT for CLK/CYC/PER/TIM complex. The biochemical meaning of the parameters is explained in Table 1.

1. Probabilities of transcription factors binding to a binding site (E-box or V/P box) in promoters:

The binding probabilities defined in the model are CLK/CYC binding to an E-box element in the *per* promoter (Pr_{cper}), in the *tim* promoter (Pr_{ct}), in the *vri* promoter (Pr_{cv}), and to the *pdp1* promoter (Pr_{cpdp}); VRI binding to a V/P box in the *clk* promoter (Pr_{vc}), and PDP1 binding to that in the *clk* promoter (Pr_{pc}). The first term in the right

side of Eq. 1 – 6 denotes binding processes, and the second term denotes unbinding processes. A detailed derivation of the probabilities is provided in the appendix.

$$d(\mathrm{Pr}_{cper})/dt = (1-\mathrm{Pr}_{cper}) \times bccper_p \times CC - \mathrm{Pr}_{cper} \times ubccper_p \quad (1)$$

$$d(\mathrm{Pr}_{ct})/dt = (1-\mathrm{Pr}_{ct}) \times bcctim_p \times CC - \mathrm{Pr}_{ct} \times ubcctim_p \quad (2)$$

$$d(\mathrm{Pr}_{cpdp})/dt = (1-\mathrm{Pr}_{cpdp}) \times bccpdp_p \times CC - \mathrm{Pr}_{cpdp} \times ubccpdp_p \quad (3)$$

$$d(\mathrm{Pr}_{cv})/dt = (1-\mathrm{Pr}_{cv}) \times bccvri_p \times CC - \mathrm{Pr}_{cv} \times ubccvri_p \quad (4)$$

$$d(\mathrm{Pr}_{vc})/dt = (1-\mathrm{Pr}_{vc}-\mathrm{Pr}_{pc}) \times bvriclk_p \times VRI - \mathrm{Pr}_{vc} \times ubvriclk_p \quad (5)$$

$$d(\mathrm{Pr}_{pc})/dt = (1-\mathrm{Pr}_{vc}-\mathrm{Pr}_{pc}) \times bpdpclk_p \times PDP - \mathrm{Pr}_{pc} \times ubpdpclk_p \quad (6)$$

2. mRNAs of *per*, *tim*, *clk*, *vri* and *pdp1*:

The first three terms in the right side of Eq. 7 and the first two terms in that of Eq. 8 – 11 describe the transcriptional processes, which are explained in detail in the appendix; the last term in these equations describes the degradation processes of mRNAs.

$$\begin{aligned} d(clk_m)/dt = {} & \mathrm{Pr}_{vc} \times tcvriclk_p + \mathrm{Pr}_{pc} \times tcpdpclk_p + (1-\mathrm{Pr}_{vc}-\mathrm{Pr}_{pc}) \times tcclk_p \\ & - dclkm \times clk_m \end{aligned} \quad (7)$$

$$d(per_m)/dt = (1-(1-\mathrm{Pr}_{cper})^{npt}) \times tcccper_p + (1-\mathrm{Pr}_{cper})^{npt} \times tcdvpmt - dperm \times per_m \quad (8)$$

$$d(tim_m)/dt = (1-(1-\mathrm{Pr}_{ct})^{npt}) \times tccctim_p + (1-\mathrm{Pr}_{ct})^{npt} \times tcdvpmt - dtimm \times tim_m \quad (9)$$

$$d(vri_m)/dt = (1-(1-\mathrm{Pr}_{cv})^{nvri}) \times tcccvri_p + (1-\mathrm{Pr}_{cv})^{nvri} \times tcdvpmt - dvrim \times vri_m \quad (10)$$

$$d(pdp_m)/dt = (1-(1-\mathrm{Pr}_{cp})^{npdp}) \times tcccpdp_p + (1-\mathrm{Pr}_{cp})^{npdp} \times tcdvpmt - dpdpm \times pdp_m \quad (11)$$

3. PER, TIM, CLK, VRI and PDP1 proteins:

The first term in the right side of Eq. 12 – 16 expresses the transcriptional processes, and the last term expresses the degradation processes of proteins. The second term in that of Eq. 12 – 14 denotes the association of complexes, and the third term denotes the dissociation of complexes.

$$d(PER)/dt = tlper \times per_m - bpt \times PER \times TIM + ubpt \times PT - dper \times PER \quad (12)$$

$$d(TIM)/dt = tltim \times tim_m - bpt \times PER \times TIM + ubpt \times PT - dtim \times TIM \quad (13)$$

$$d(CLK)/dt = tlclk \times clk_m - bcc \times CLK + ubcc \times CC - dclk \times CLK \quad (14)$$

$$d(VRI)/dt = tlvri \times vri_m - dvri \times VRI \quad (15)$$

$$d(PDP)/dt = tlpdp \times pdp_m - dpdp \times PDP \quad (16)$$

4. PER/TIM, CLK/CYC and PER/TIM/CLK/CYC complexes:

The first and second terms in Eq. 17 – 19 describe the association and dissociation of PT, CC and CCPT complexes, respectively, and the last term describes the degradation

processes of these complexes. The third and fourth terms in Eq. 17 – 18 denote the association and dissociation of CCPT complex.

$$d(PT)/dt = bpt \times PER \times TIM - ubpt \times PT - bccpt \times PT \times CC + ubccpt \times CCPT - dpt \times PT \quad (17)$$

$$d(CC)/dt = bcc \times CLK \times CYC - ubcc \times CC - bccpt \times PT \times CC + ubccpt \times CCPT - dcc \times CC \quad (18)$$

$$d(CCPT)/dt = bccpt \times PT \times CC - ubccpt \times CCPT - dccpt \times CCPT \quad (19)$$

3.3. Parameters and initial conditions

Experimental data to estimate parameter values are lacking. Although some information is available about the relationship between the transcription, translation and degradation of mRNAs and proteins rates in the circadian clock in plants (Shu and Hong-Hui 2004), no quantities for the rates have been determined. Therefore, to obtain appropriate values for the parameters in the model, it is necessary to rely on trial-and-error validation. Criteria for parameter estimation are that the model should produce sustained circadian oscillations of mRNAs and proteins, correct measured phase relationships between gene expression and proteins, and appropriate time delays between mRNAs and proteins under the condition of constant darkness. In addition, circadian oscillations should be robust in respect to parameter variations. Because this set of parameters remains unchanged during most of simulations, with exceptions noted in the text, we call this set the “standard parameters”. The standard parameters are shown in Table 1. Time is in hourly units. Concentrations are referenced to the total cell volume, and are in units of nM.

(Table 1**)**

Because the system governed by Eq. (1) to (19) can maintain sustained, periodic oscillations using the standard set of parameters regardless of initial conditions, the initial conditions have no influence on the final state of the system. However, to eliminate the transient dynamics from the initial state to the stable oscillation state, we use the initial conditions listed in Table 2. The concentrations for each gene are constant. Additionally, as explained above, the concentration of CYC is also assumed to be constant. These fixed values are listed in Table 2 and remarked by a '*'.

(Table 2)

4. Simulation methods and results

All simulations were done using Matlab and 'ode15s' function was used to numerically solve the equations (The MathWorks, Natick, MA, U.S.A). The simulations were also verified by CellDesigner (Funahashi 2003). The analysis of parameter sensitivity was performed with SBtoolbox (Schmidt and Jirstrand 2005). The SBML format file of the model is available upon request.

4.1. Circadian oscillations in constant darkness (DD)

For simulations under conditions of DD, the parameters did not change in the course of time. Numerical solution of the model showed sustained oscillations with 24 h period in the concentrations of *per*, *tim*, *vri*, *pdp1* and *clk* mRNAs and their corresponding proteins using the standard parameter set given in Table 1.

Oscillations in mRNA concentrations from the simulation were plotted in Figure 3A. The oscillations of *per* and *tim* mRNAs are in phase and their levels peak at circadian time (CT)12. The oscillation of *clk* mRNA is in anti-phase with *per* and *tim* mRNAs; it peaks at CT3 and subsequently bottoms in CT13.5. These results are consistent with observations that *per* and *tim* mRNA levels oscillate in phase to one another and they

reach peak levels early in the evening at CT12 – CT16 (Hardin, Hall et al. 1990); *clk* mRNA levels oscillate in anti-phase to *per* and *tim* mRNA levels and *clk* mRNA levels peak at late night to early in the morning (CT23 – CT4) (Bae, Lee et al. 1998); the simulated concentration of *vri* mRNA reaches a peak at CT11.5 and that of *pdp1* mRNA reaches its maximum at CT13.5 with a 2 h delay. This agrees with experimental data that *vri* mRNA oscillates in anti-phase with *clk* mRNA, and *pdp1* mRNA oscillates with a similar phase to *vri* mRNA after several hours delay (Cyran, Buchsbaum et al. 2003; Glossop, Houl et al. 2003).

Figure 3B illustrates the oscillations in concentrations of proteins. On the one hand, the peaks of PER and TIM concentrations are at CT15, the peak of VRI concentration is at CT12 and that of PDP1 is at CT18. On the other hand, the concentration of CLK peaks at CT4.5 and bottoms at CT14.5. *In vitro* experimental data showed that protein levels of PER and TIM are at their highest in the middle of the night with 4 h – 6 h delay to their mRNA peaks (Zeng, Qian et al. 1996), and a lag of 3 h – 6 h exists between the rise of VRI and that of PDP1 (Cyran, Buchsbaum et al. 2003). The phase of the maximum and minimum from the simulated results are all in good agreement with the experimental observations.

(Figure 3**)**

4.2. Robustness to parameter variations

Robustness is the ability of a system to maintain its functionality across a range of operational conditions. Robustness for cells means that cells can function normally with modest environmental changes, which might cause variability in concentrations of cellular components and in parameters of cellular biochemical reactions. Biochemical parameters may be also vary from individual cell to cell due to intrinsic differences from each other. The circadian clock is known to have the ability of regulating the phase relationships of different physiological processes in a daily cycle. Normally, it should maintain circadian rhythms with a period close to 24 h regardless of parameter

variations. It has been reported that there is only 0.1 h variation from the mean value of 24.3 h for wild-type (WT) flies (Levine, Funes et al. 2002). In another report, 0.06 h variation from the mean value has been found at $29^{o}C$, and 0.1 and 0.2 h variations at $20^{o}C$ and $25^{o}C$, respectively (Bao, Rihel et al. 2001). It should be noted that under $20^{o}C$ and $25^{o}C$, there are non-negligible percentages of flies appearing arrhythmic (4/15 and 3/20, respectively). Therefore in a model of the circadian clock, modest parameter variations should only result in minor period changes given that arrhythmic flies are not considered.

As there are 44 parameters to be tested (not including three parameters for the number of E-boxes in promoters), it is not possible to explore the behaviour of the system in full dimensional parameter spaces. To investigate the behaviour of the system to parameter variations, we followed the methods used in previous models (Lema, Golombek et al. 2000; Leloup and Goldbeter 2003; Smolen, Hardin et al. 2004). One parameter was changed at a time while keeping the others at their standard values. Perturbations were simulated by increasing or decreasing 20% from its standard value for each individual parameter.

Oscillations were preserved in all the simulations. From Figure 4 we can see that the periods vary less than 0.8 h from the control values of 24 h with 20% perturbation to each parameter. The largest period increase (+0.75 h) is caused by increase in binding rate of PDP1 to *clk* promoter. The largest two periods of decrease are very close (-0.8 h), and are caused by a decrease in binding rates of CLK/CYC to *pdp1* and *per* promoters. In comparison with previous models using Michaelis-Menten kinetics (Leloup and Goldbeter 2003; Smolen, Hardin et al. 2004), our model had a less period variation.

(Figure 4**)**

4.3. Response of the circadian clock to light

On the one hand, the circadian clocks are robust to parameter variations, on the other hand, a fundamental characteristic of the circadian clocks is that they are also entrained (phase-adjusted) by Zeitgeber (Zeitgeber means “time giver”, it provides an environmental time cue). This entrain-ability gives the circadian systems a proper phase in synchrony with the outside world. Although both ambient light and temperature cycles on a daily basis, light is often thought to be the predominant Zeitgeber. Here we test the entrain-ability of our circadian clock model in response to light.

Entrainment by light is generally considered by changing particular parameters in the circadian clocks. In *Drosophila*, it has been shown experimentally that light enhances degradation of TIM, and consequently degradation of TIM in the light alters the level of other clock components and, thus, resets of phase of a oscillator (Zeng, Qian et al. 1996). In terms of modelling, increase in TIM degradation rate has been used to model light response and entrainment to LD cycles in some previous models (Leloup and Goldbeter 1998; Tyson, Hong et al. 1999). As TIM stabilises PER in the cytoplasm, the indirect effect of light is to regulate the localisation of PER and in turn to decrease the PER level in the nucleus. Therefore, change in degradation rate of PER has also been used in some models (Scheper, Klinkenberg et al. 1999; Lema, Golombek et al. 2000; Smolen, Hardin et al. 2004). Indeed, experimental findings have shown that tim^{01} mutants inducing an absence of TIM lead to a substantial lowering of PER abundance (Vosshall, Price et al. 1994; Price, Dembinska et al. 1995), an effect that happens to be similar to the result of exposing flies to constant light (Zerr, Hall et al. 1990; Price, Dembinska et al. 1995). Because we did not include the detailed translocation mechanisms of PER and TIM into the nucleus, as well as associated Sgg-dependent TIM phosphorylation and CK2-dependent PER phosphorylation processes in the model (Shafer, Rosbash et al. 2002), we simulated the effect of light by increasing the degradation rates of both TIM and PER. Consequently, a new parameter k_{light} replaced dtim and dper to denote the new degradation rates.

To model entrainment to LD cycles we used a higher value of k_{light} (> 0.62) in the light phase at Zeitgeber time (ZT) 0 – ZT12, and restored its original dark value (0.62) during the dark phase ZT12 – ZT24. The value of k_{light} during light phase was

arbitrarily chosen. Figure 5A shows that oscillations in all proteins are maintained during entrainment by LD. The phase and anti-phase relationship between mRNAs and proteins (data not shown) were also maintained as in condition of DD. Simulations have shown that the phase changes are dependent upon the magnitude of k_{light} during light exposure. For ease of comparison in the phase changes, we plotted CLK concentration using different k_{light} values in Figure 5B, which shows the phases have been delayed for several hours depending on the different k_{light} values we chose.

As shown experimentally, disappearance of the rhythmicity in flies in constant light (LL) can also be simulated by holding k_{light} at a high constant value. It was found that the oscillations were damped in LL when k_{light} value was close or more than five. We plotted the damped protein oscillations using a k_{light} value of five in Figure 5C.

(Figure 5**)**

Next we investigated the oscillatory behaviour of the clock model under influence of light pulse. Phase responses were simulated by applying a 2 h duration light pulse to the system at different time points during the free-running conditions of DD. Two hours duration was chosen since normally 1 – 4 h duration was used in previous models (Leloup, Gonze et al. 1999; Smolen, Hardin et al. 2004). The phase shifts were determined from the difference in the maximum values of a specified protein between the free-running system and the perturbed system. Because all the proteins oscillate with a same period, the choice of protein should not make any difference to the phase shifts. The phase shifts were measured after the transient effect of the light pulse was over. This procedure was applied 24 times by increasing one hour in the time of application of the light pulse each time. Phase response curve (PRC) was determined by plotting the phase shifts as a function of the circadian time at which perturbation was applied. We defined CT0 – CT12 as subjective day and CT12 – CT24 as subjective night.

Similar to the simulations of entrainment by LD, the effect of light pulse was simulated by replacing degradation rates of PER and TIM by k_{light}. Simulations showed that the

magnitude of the phase shifts varied depending on the value of $k_{light.}$ The bigger the value, the more significant phase shifts obtained (data not shown). The best fit with experimental PRC was obtained by using klight=1.3 as plotted in Figure 6. Like the PRC plot in Smolen et al. (2004), the mean value of the PRC obtained by Konopka et al. (1991) was also plotted for comparison.

From Figure 6, it is shown that the simulated data show a consistent 5 h time lag from the experimental data. To clearly compare the actual values of the theoretical PRC from our model with the PRC obtained from the *in vitro* experimental, we shifted the simulated PRC by advancing it by 5 h. The reason of a 5 h lag between the theoretical (simulated) PRC and the experimental PRC could be that we did not include phosphorylation of PER and TIM and the separate nuclear and cytoplasmic compartments in the model. However, phosphorylation and nuclear entry of PER and TIM provide an important time delay between cytoplasmic PER and TIM and nuclear PER/TIM. This time delay also implies a time lag between the effects of light and the repression of CLK/CYC by PER/TIM, which is not presented in the current model.

(Figure 6**)**

4.4. Mutations

A number of mutations that influence circadian rhythms have been reported in *Drosophila*. Mutations can be readily simulated in the model by changing particular parameters according to the functionality of mutants while keeping the rest of parameters as in the standard set.

We first explored E-box mutations. As explained in Section 2, we use the number of E-boxes of five in the *per* and *tim* genes, six in the *pdp1* gene and four in the *vri* gene. Here we reduced the number of E-boxes in one gene and kept the others unchanged for a single E-box mutation. We also reduced the number of E-boxes in more than one gene simultaneously for multiple E-boxes mutations. In all the simulations, oscillations in

concentrations of all the mRNAs and proteins were preserved with a shorter period and at lower amplitudes. The periods of the oscillations and the amplitudes of the phases were reduced by different extents for different E-box mutations. Figure 7 shows mRNA oscillations where only one copy of E-box exists in each gene. The phase and anti-phase relationship between mRNAs are maintained and the period of oscillations (22.5 h) is close to WT, as shown in Figure 3. The notable difference between the E-box mutation and WT is that the transcription levels of all the genes are reduced. This is consistent with experimental observations that the rhythmic *per* and *tim* transcription are remained in E-box mutations, although the transcription level is reduced (McDonald and Rosbash 2001).

(Figure 6)

Next we tested some arrhythmic mutants. In *Drosophila* per^{01}, tim^{01} and clk^{Jrk} refer to null mutations in *per*, *tim* and *clk* genes which produce non-functional proteins. These mutations were simulated by setting the translation rates of their respective proteins to zero. Figure 8 illustrates that sustained oscillations are abolished in per^{01}, tim^{01} and clk^{Jrk}. The results are consistent with the reports that rhythmicity of *per*, *tim* and *clk* mRNAs is blocked in per^{01}, tim^{01} and clk^{Jrk} (Bae, Lee et al. 1998), and oscillations in *pdp1* and *vri* mRNA levels are also blocked by these mutations (Cyran, Buchsbaum et al. 2003). However some simulated mRNA levels, particularly *per* and *tim*, greatly differ from the experimental reports. Experiments have shown that in mutants lacking PER (per^{01}) and TIM (tim^{01}), *per* and *tim* mRNA levels are constitutive and low (So and Rosbash 1997); *vri* mRNA levels are at intermediate (Blau and Young 1999); *pdp1* mRNA levels are high (Cyran, Buchsbaum et al. 2003); and the levels of *clk* mRNA are low (Glossop, Lyons et al. 1999). The simulated results show high levels of *per*, *tim*, *vri* and *pdp1* mRNAs and a low level of *clk* mRNA (Figure 8A). These results can be explained by the structure of the model: per^{01} and tim^{01} induced absences of PER and TIM lead to a loss of PER/TIM, which, in turn, causes a very high level of CLK. As the activation effects of CLK/CYC, *per*, *tim*, *vri* and *pdp1* mRNAs are all higher than their peaks in WT. Consequently, high concentrations of VRI and PDP1 are produced. Because we have assumed that VRI has a stronger binding ability to the *clk* promoter

than PDP1 (probabilities of VRI and PDP1 binding to the *clk* promoter are 0.65574 and 0.304181 in this condition from calculation), strong repression from VRI makes a low level of *clk* mRNA.

In clk^{Jrk} flies, experimental data have shown low levels of *per*, *tim*, *vri* and *pdp1* mRNAs (Allada, White et al. 1998; Cyran, Buchsbaum et al. 2003), and a high level of *clk* mRNA which is near the WT peak (Glossop, Lyons et al. 1999). The simulated data (Figure 8B) agree in terms of the low levels of *per*, *tim*, *vri* and *pdp1* mRNAs, but show a disparity in the low level of *clk* mRNA. The mechanism underlying these resulting data from the model can be explained as follows. Because of the absence of activation effects which are from functional CLK, low levels of *per*, *tim*, *vri* and *pdp1* mRNAs are produced. Consequently, low levels of PER, TIM, VRI and PDP1 follow. A small amount of *clk* mRNA is present because the repression effect from VRI is higher than the activation effect from PDP1 under the assumptions of this model.

(Figure 8**)**

In vitro experiments, besides arrhythmic mutants in *Drosophila*, a number of short and long mutants also have been observed. For example, per^L mutants lengthen the free-running periods to 29 h and per^S mutants shorten the free-running periods to 19 h (Konopka and Benzer 1971). It was suggested in a previous theoretical study that *Drosophila's* per^S and per^L mutants can be modelled computationally by altering stability of the PER protein or PER-protein interactions (Ruoff and Rensing 1996). In our model, per^S mutants were simulated by setting a enhanced rate of degradation of the PER/TIM dimmer (dpt) according to the results from Curtin el al. (1995). Similar to the simulations carried out by Ruoff et al. (2005), per^L mutants were represented by increasing in the PER/TIM stability although this has not been experimentally confirmed. Figure 9 shows the PER plots of per^S and per^L mutants with a period of 19 h and 29 h where the degradation rate of PER/TIM was set to 0.9 and 0.08, respectively. *In vitro* experiments, it has been shown that nuclear entry of PER is delayed in the three per^L types compared with that in WT flies (Curtin, Huang et al. 1995; Lee, Parikh et al. 1996) and a larger proportion of PER^S are phosphorylated at an earlier time in the morning than PER in per^S mutants (Edery, Zwiebel et al. 1994). However, as the current

model does not include phosphorylation of PER and separation of the nucleus and the cytoplasm, we intend to simulate these experimental findings in a more complete model in future.

5. Discussion

In this research we have presented a model for the circadian clock in *Drosophila* incorporating the key clock component genes identified so far. This model has unique properties compared with most previous models. (1) The model incorporates the transcriptional regulation of the *per*, *tim*, *vri*, *pdp1* and *clk* genes. (2) Conventional Hill functions to describe the regulation of gene expression are not assumed in the model; this paves the way to study for transcriptional regulation in the circadian clock at a more detailed level. (3) First-order reactions are used to describe translation and degradation processes; this makes the model simple and easy to analyse.

Using a set of parameters, the model produces autonomous sustained oscillations in conditions corresponding to constant darkness. The simulated results show right phases of all the components in the system, correct phase and anti-phase relationship of mRNAs and proteins, as well as appropriate lags between mRNAs and proteins. These are in good agreement with experimental data. The model also accounts for the disappearance of the oscillations in constant light.

Robustness is an important characteristic of the circadian clock, which should produce close to 24 h periodic oscillations regardless of modest variations in parameters under certain conditions. We have measured the variations in period by increasing and decreasing each parameter 20% at a time. The oscillatory patterns remain in all the cases with the largest period variation being around 0.8 h for 20% parameter perturbations. Parameter sensitivity analysis has suggested that several of the most sensitive parameters are binding rate of PDP1 to *clk* promoter, and binding rates of CLK/CYC to *pdp1* and *per* promoters. These are all positive elements in the network.

It is also essential that the circadian clock should have the ability to reset phases in response to Zeitgeber, where light is the most important. We have simulated the effect of light by increasing the degradation rates of TIM and PER. Simulations have shown the entrainment of the system by LD cycles and the induction of phase shifts by light pulses. In the entrainment by LD, the phase relationship in mRNAs and proteins are well maintained with a period of 24 h and the phase of oscillations is delayed depending on the particular degradation rates we chose. We have also constructed a phase-response curve to represent the phase shifts induced by temporal promotion of TIM and PER degradation. When shifting the simulated PRC by advancing it for 5 h, the agreement between the shifted and experimental PRCs appears very good. Both data show a dead zone in the middle of the subjective day, a phase delay during the early subjective night, and a phase advance during the late subjective night. The time lag between the simulated and the experimental data suggests that some unpresented mechanisms in the model, such as phosphorylation and nuclear entry of TIM and PER, are important to provide a time delay in response to light.

We also have carried out a number of tests for simulating mutations. Mathematical mutants are simulated by setting an appropriate parameter value according to the functionality of mutants. The simulated short and long mutants, per^S and per^L , resemble their phenotypes where 19 h and 29 h of period are found, respectively. In arrhythmic mutants, oscillations of all the mRNAs and proteins are blocked in per^{01}, tim^{01} and clk^{Jrk} as shown in experiments. However, some mRNAs levels differ significantly from the experimental data. In particular simulated data have shown high levels of *per* and *tim* mRNA in per^{01} and tim^{01} and low level of *clk* mRNA in clk^{Jrk}, which are opposite values to those found in the experiments. This deficiency obviously comes from the structure of the model, as discussed previously. In the model we assume that the *per*, *tim*, *vri*, and *pdp1* promoters are all strongly activated by CLK/CYC. The low levels of *per* and *tim* mRNAs in per^{01} and tim^{01} cannot be explained by this model because the loss of PER/TIM directly results in a high level of CLK and, consequently, high levels of *per* and *tim* mRNAs. Furthermore, although the assumption of strong binding ability of VRI to CLK gives a reasonable low level of *clk* mRNA in per^{01} and tim^{01}, this assumption nevertheless produces a low level of *clk* mRNA in clk^{Jrk}, which is, again, different from the experimental observations in which a high level of *clk* mRNA is found. The

deficiency of the model could indicate the possibility of unknown part in the genetic regulatory network of the circadian clock in *Drosophila*.

An important property of the model, which distinguishes it from the previous models, is the way that the regulation of transcription processes is modelled. In previous models, transcriptional regulation was modelled by Hill functions without explicit descriptions of binding and unbinding processes of transcription factors to E-boxes elements in promoters (Allada, White et al. 1998; Leloup and Goldbeter 1998; Glossop, Lyons et al. 1999; Ueda, Hagiwara et al. 2001; Smolen, Hardin et al. 2004). Hill cooperativity coefficient may correspond to the number of binding sites of genes (Hill 1910; Segel 1993). Different models used different Hill cooperativity coefficients to make sustained oscillations. The exact value of the minimum cooperativity coefficients depends on the choice of the model structure and model parameters. In most of the previous models, a Hill coefficient of more than one was used to describe the activation of *per* expression by CLK or repression of *per* expression by PER to create oscillations, whereas in some models it was found that oscillations were preserved with a Hill coefficient of one if other parameters were properly chosen (Leloup and Goldbeter 1998; Tyson, Hong et al. 1999; Kurosawa, Mochizuki et al. 2002). Using the explicit description of transcription factors binding to promoters and activating or repressing gene expressions, our model can readily take account of different binding sites and cooperativity. The simulation has shown that even with one E-box in *per*, *tim*, *vri* and *pdp1* promoters, oscillations are preserved with reduced transcription levels in agreement with *in vitro* experiments that only one copy of E-box does not abolish rhythmic *per* and *tim* transcription, although the transcription levels are reduced (McDonald and Rosbash 2001).

Finally, we would like to make some comparisons with two previous models as the core mechanisms of these models are similar (Smolen, Hardin et al. 2004; Ruoff, Christensen et al. 2005). All the models contain two interlocked transcription and translation feedback loops where, on the one hand, PER represses its own gene expression by binding to its activator CLK and, on the other hand, VRI and PDP1 regulate the gene expression of *clk*.

In the model proposed by Ruoff et al. (2005), the core mechanism is that VRI and PDP1 regulate *clk* expression with negative and positive feedback loops and CLK, the product of *clk* expression, activates *vri*, *pdp1* and *per*/*tim* (two genes were combined) expression. The simulation showed that VRI and PDP1 feedback loops generated sustained oscillations even in the absence of PER/TIM. Therefore, the authors concluded that positive and negative feedback loops of VRI and PDP1 were essential for the overall oscillations, whereas PER/TIM played a role in amplification and stabilization of the oscillations. This result is in contrast to the findings from the model proposed by Smolen et al. (2004) in which the PER feedback loop was found to be crucial for oscillations. Ruoff et al. (2005) suggested that the discrepancy of the findings may be because Smolen's model used differential equations with delay terms where delay terms alone can generate oscillation. In our model, per^{01} and tim^{01} mutants suggested that PER and TIM are required for the oscillations of all the mRNAs and proteins, and removal of VRI and/or PDP1 feedback loops did not remove rhythmicity of *per*, *tim* and *clk* expression. Our findings confirm the roles of the PER/TIM and VRI/PDP1 feedback loops made by Smolen et al. using a different model without delay terms involved.

The main difference in terms of model representation between Smolen's and the present model is that different assumptions are used to capture the essence of various interactions. Smolen's model uses Hill functions and Michaelis-Menten rate expression describing transcriptional activation and phosophorylation processes, and discrete time delay terms are included in the equations to describe the time lags between proteins. Our model takes account of binding and unbinding processes of transcription factors to promoters but ignores the nuclear entry of proteins and phosophorylation of PER. However, the simulated results of two models are very similar regarding oscillations in constant darkness, photic entrainment of oscillations, the PRC and null mutations of *per* and *clk*. Nevertheless different predictions are made by two models. For example, E-box mutations are readily simulated in our model whereas some short and long period mutants are observed in Smolen's model. This confirms the statement made by Murray James (2002) that different mathematical models might be able to create similar behaviours and they are mainly distinguished by the different predictions they suggest and how close they are to the real biology. As both models have been simplified to some

extent from the real network, we expect that a more sophisticated model should be developed in future as more data emerge from experiments.

In summary, we have presented a circadian clock model to represent biochemical mechanisms responsible for the circadian rhythms in *Drosophila* for simulating free-running periods, entrainment to light, phase responses and mutants. This model can provide a means to investigate the complicated genetic regulatory network of the circadian clock. Some possible improvements of the present study are: (1) inclusion of more detailed post-transcriptional and post-translational regulations, such as phosphorylation of proteins; (2) inclusion of separate compartments in an extended model; (3) conversion to stochastic models to explore stochastic effects in terms of internal noise and external perturbations.

References

Allada, R., N. E. White, et al. (1998). "A mutant Drosophila homolog of mammalian Clock disrupts circadian rhythms and transcription of period and timeless." Cell **93**(5): 791-804.

Bae, K., C. Lee, et al. (1998). "Circadian regulation of a Drosophila homolog of the mammalian Clock gene: PER and TIM function as positive regulators." Mol Cell Biol **18**(10): 6142-6151.

Bao, S., J. Rihel, et al. (2001). "The Drosophila double-timeS mutation delays the nuclear accumulation of period protein and affects the feedback regulation of period mRNA." J Neurosci **21**(18): 7117-7126.

Blau, J. and M. W. Young (1999). "Cycling vrille expression is required for a functional Drosophila clock." Cell **99**(6): 661-671.

Curtin, K. D., Z. J. Huang, et al. (1995). "Temporally regulated nuclear entry of the Drosophila period protein contributes to the circadian clock." Neuron **14**(2): 365-72.

Cyran, S. A., A. M. Buchsbaum, et al. (2003). "vrille, Pdp1, and dClock form a second feedback loop in the Drosophila circadian clock." Cell **112**(3): 329-41.

Dunlap, J. C. (1999). "Molecular bases for circadian clocks." Cell **96**(2): 271-90.

Edery, I., L. J. Zwiebel, et al. (1994). "Temporal phosphorylation of the Drosophila period protein." Proc Natl Acad Sci U S A **91**(6): 2260-4.

Endy, D. and R. Brent (2001). "Modelling cellular behaviour." Nature **409**(6818): 391-5.

Etchegaray, J.-P., C. Lee, et al. (2003). "Rhythmic histone acetylation underlies transcription in the mammalian circadian clock." Nature **421**(6919): 177-182.

Ewer, J., B. Frisch, et al. (1992). "Expression of the period clock gene within different cell types in the brain of Drosophila adults and mosaic analysis of these cells' influence on circadian behavioral rhythms." J Neurosci **12**(9): 3321-3349.

Forger, D. B. and C. S. Peskin (2003). "A detailed predictive model of the mammalian circadian clock." Proc Natl Acad Sci U S A **100**(25): 14806-11.
Funahashi, A., Tanimura, N., Morohashi, M., and Kitano, H. (2003). " CellDesigner: a process diagram editor for gene-regulatory and biochemical networks." Biosilico **1**: 159-162.
Glossop, N. R., L. C. Lyons, et al. (1999). "Interlocked feedback loops within the Drosophila circadian oscillator." Science **286**(5440): 766-8.
Glossop, N. R. J., J. H. Houl, et al. (2003). "Vrille feeds back to control circadian transcription of Clock in the Drosophila circadian oscillator." Neuron **37**(2): 249-261.
Goldbeter, A. (1995). "A model for circadian oscillations in the Drosophila period protein (PER)." Proc R Soc Lond B **261**(1362): 319-24.
Goldbeter, A. (2002). "Computational approaches to cellular rhythms." Nature **420**(6912): 238-45.
Hardin, P. E. (2005). "The circadian timekeeping system of Drosophila." Current Biology **15**(17): R714-R722.
Hardin, P. E., J. C. Hall, et al. (1990). "Feedback of the Drosophila period gene product on circadian cycling of its messenger RNA levels." Nature **343**(6258): 536-40.
Hida, A., N. Koike, et al. (2000). "The human and mouse Period1 genes: five well-conserved E-boxes additively contribute to the enhancement of mPer1 transcription." Genomics **65**(3): 224-33.
Hill, A. V. (1910). "The possible effects of the aggregation of the molecules of haemoglobin on its oxygen dissociation curve." J Physiol **40**: 4-7.
Kitano, H. (2002). "Systems biology: a brief overview." Science **295**(5560): 1662-1664.
Konopka, R. J. and S. Benzer (1971). "Clock mutants of Drosophila melanogaster." Proc Natl Acad Sci U S A **68**(9): 2112-6.
Kurosawa, G., A. Mochizuki, et al. (2002). "Comparative study of circadian clock models, in search of processes promoting oscillation." J Theor Biol **216**(2): 193-208.
Lee, C., K. Bae, et al. (1998). "The Drosophila CLOCK protein undergoes daily rhythms in abundance, phosphorylation, and interactions with the PER-TIM complex." Neuron **21**(4): 857-67.
Lee, C., V. Parikh, et al. (1996). "Resetting the Drosophila clock by photic regulation of PER and a PER-TIM complex." Science **271**(5256): 1740-4.
Leloup, J.-C. and A. Goldbeter (2003). "Toward a detailed computational model for the mammalian circadian clock." PNAS **100**(12): 7051-7056.
Leloup, J. C. and A. Goldbeter (1998). "A model for circadian rhythms in Drosophila incorporating the formation of a complex between the PER and TIM proteins." J Biol Rhythms **13**(1): 70-87.
Leloup, J. C., D. Gonze, et al. (1999). "Limit cycle models for circadian rhythms based on transcriptional regulation in Drosophila and Neurospora." J Biol Rhythms **14**(6): 433-48.
Lema, M. A., D. A. Golombek, et al. (2000). "Delay model of the circadian pacemaker." J Theor Biol **204**(4): 565-73.
Levine, J. D., P. Funes, et al. (2002). "Signal analysis of behavioral and molecular cycles." BMC Neurosci **3**: 1.
McDonald, M. J. and M. Rosbash (2001). "Microarray analysis and organization of circadian gene expression in Drosophila." Cell **107**(5): 567-78.
Murray, J. D. (2002). Mathematical biology. New York, Springer.

Pittendrigh, C. S. (1993). "Temporal organization: reflections of a Darwinian clock-watcher." Annu Rev Physiol **55**: 16-54.
Price, J. L., J. Blau, et al. (1998). "double-time is a novel Drosophila Clock gene that regulates PERIOD protein accumulation." Cell **94**(1): 83-95.
Price, J. L., M. E. Dembinska, et al. (1995). "Suppression of PERIOD protein abundance and circadian cycling by the Drosophila clock mutation timeless." EMBO J **14**(16): 4044-9.
Ruoff, P., M. K. Christensen, et al. (2005). "PER/TIM-mediated amplification, gene dosage effects and temperature compensation in an interlocking-feedback loop model of the Drosophila circadian clock." J Theor Biol **237**(1): 41-57.
Ruoff, P. and L. Rensing (1996). "The temperature-compensated Goodwin model simulates many circadian clock properties." J Theor Biol **179**(4): 275-285.
Scheper, T., D. Klinkenberg, et al. (1999). "A mathematical model for the intracellular circadian rhythm generator." J Neurosci **19**(1): 40-7.
Schmidt, H. and M. Jirstrand (2005). "Systems Biology Toolbox for MATLAB: a computational platform for research in Systems Biology." Bioinformatics: 799.
Schoning, J. C. and D. Staiger (2005). "At the pulse of time: protein interactions determine the pace of circadian clocks." FEBS Lett **579**(15): 3246-3252.
Segel, I. H. (1993). Enzyme kinetics : behavior and analysis of rapid equilibrium and steady state enzyme systems. New York, Wiley.
Shafer, O. T., M. Rosbash, et al. (2002). "Sequential nuclear accumulation of the clock proteins period and timeless in the pacemaker neurons of Drosophila melanogaster." J Neurosci **22**(14): 5946-54.
Shu, Y. and L. Hong-Hui (2004). "Transcription, translation, degradation, and circadian clock." Biochem Biophys Res Commun **321**(1): 1-6.
Smolen, P., D. A. Baxter, et al. (2001). "Modeling circadian oscillations with interlocking positive and negative feedback loops." J Neurosci **21**(17): 6644-56.
Smolen, P., P. E. Hardin, et al. (2004). "Simulation of Drosophila circadian oscillations, mutations, and light responses by a model with VRI, PDP-1, and CLK." Biophys J **86**(5): 2786-2802.
So, W. V. and M. Rosbash (1997). "Post-transcriptional regulation contributes to Drosophila clock gene mRNA cycling." EMBO J **16**(23): 7146-55.
Tyson, J. J., C. I. Hong, et al. (1999). "A simple model of circadian rhythms based on dimerization and proteolysis of PER and TIM." Biophys J **77**(5): 2411-2417.
Ueda, H., K. Hirose, et al. (2002). "Intercellular Coupling Mechanism for Synchronized and Noise-Resistant Circadian Oscillators." Journal of Theoretical Biology **216**(4): 501-512.
Ueda, H. R., M. Hagiwara, et al. (2001). "Robust oscillations within the interlocked feedback model of Drosophila circadian rhythm." J Theor Biol **210**(4): 401-6.
Van Gelder, R. N., E. D. Herzog, et al. (2003). "Circadian rhythms: in the loop at last." Science **300**(5625): 1534-1535.
Vilar, J. M., H. Y. Kueh, et al. (2002). "Mechanisms of noise-resistance in genetic oscillators." Proc Natl Acad Sci U S A **99**(9): 5988-92.
Vosshall, L. B., J. L. Price, et al. (1994). "Block in nuclear localization of period protein by a second clock mutation, timeless." Science **263**(5153): 1606-9.
Yamaguchi, S., S. Mitsui, et al. (2000). "The 5' upstream region of mPer1 gene contains two promoters and is responsible for circadian oscillation." Curr Biol **10**(14): 873-6.
Young, M. W. and S. A. Kay (2001). "Time zones: a comparative genetics of circadian clocks." Nat Rev Genet **2**(9): 702-15.

Yu, W., H. Zheng, et al. (2006). "PER-dependent rhythms in CLK phosphorylation and E-box binding regulate circadian transcription." Genes Dev **20**(6): 723-733.
Zeng, H., Z. Qian, et al. (1996). "A light-entrainment mechanism for the Drosophila circadian clock." Nature **380**(6570): 129-35.
Zerr, D. M., J. C. Hall, et al. (1990). "Circadian fluctuations of period protein immunoreactivity in the CNS and the visual system of Drosophila." J Neurosci **10**(8): 2749-62.

Appendix

1. Probabilities of CLK/CYC binding to E-boxes in *per*, *tim*, *vri* and *pdp1* promoters and transcription rates of their genes

Suppose there are *n* E-boxes in a promoter where CLK/CYC dimers can bind. Since we assume that CLK/CYC dimers bind to individual E-box independently, we can consider each E-box separately. The binding and unbinding processes of CLK/CYC to an E-box can be formulated below:

$$B + T \underset{ub_{bt}}{\overset{b_{bt}}{\rightleftharpoons}} BT\ , \tag{20}$$

where B is the binding site, i.e. an E-box; T is the transcription factor CLK/CYC; and BT denotes CLK/CYC bound to the E-box; b_{bt} is rate of CLK/CYC binding to the E-box and ub_{bt} is the rate of CLK/CYC releasing from the E-box. We can get Eq. (21) using mass-action kinetics,

$$d[BT]/dt = [B][T]\,b_{bt} - [BT]\,ub_{bt}\,. \tag{21}$$

Suppose the volume of the cell is V. The number of B and BT in the cell are $[B]V$ and $[\mathrm{BT}]V$. Since the total number of B and BT, is *n*, then we get

$$d[BT]/dt = ((n/V) - [BT])\,[T]\,b_{bt} - [BT]\,ub_{bt}\,. \tag{22}$$

Let Pr_{bt} be the number of occupied E-boxes over the total number of E-boxes. [BT] = Total number of E-boxes$/V \times \mathrm{Pr}_{bt}$. Since the total number of E-boxes is *n*, Eq. (22) becomes

$$d((n/V)\,\mathrm{Pr}_{bt})/dt = ((n/V) - (n/V)\,\mathrm{Pr}_{bt})\,[T]\,b_{bt} - (n/V)\,\mathrm{Pr}_{bt}\,ub_{bt}. \qquad (23)$$

Simplify it to

$$d\,\mathrm{Pr}_{bt}/dt = (1 - \mathrm{Pr}_{bt})\,[T]\,b_{bt} - \mathrm{Pr}_{bt}\,ub_{bt}. \qquad (24)$$

Now we can calculate probabilities for CLK/CYC binding to the whole promoter in a gene. Assume CLK/CYC can bind independently to any of *n* E-boxes and if one or more E-boxes are bound, transcription of that gene is activated at a rate tc_{av} otherwise at a deactivated rate tc_{dvpmt}. The probability of none of E-boxes being bound is $(1-\mathrm{Pr}_{bt})^n$. The rate of transcription would then be

$$tc_{av}\;\;(1-(1-\mathrm{Pr}_{bt})^n) + tc_{dvpmt}(1-\mathrm{Pr}_{bt})^n. \qquad (25)$$

2. Probabilities of VRI and PDP1 binding to V/P box in *clk* promoter and transcription rate of *clk* gene

Assume there is only one binding site B, i.e. V/P box, in the *clk* promoter and an activator PDP1, denoted by A, and a repressor VRI, denoted by R, compete to bind that site. We write the reactions as below:

$$B + A \underset{ub_{ba}}{\overset{b_{ba}}{\rightleftharpoons}} BA; \qquad (26)$$

$$B + R \underset{ub_{br}}{\overset{b_{br}}{\rightleftharpoons}} BR. \qquad (27)$$

Where b_{ba} is rate of PDP1 binding to the V/P box, and ub_{ba} is rate of PDP1 releasing from V/P box; b_{br} is rate of VRI binding to the V/P box, and ub_{br} is rate of VRI releasing from V/P box. We can get Eq. (26) and (27) simply using mass-action kinetics:

$$d[BA]/dt = [B][A]\,b_{ba} - [BA]\,ub_{ba}; \tag{28}$$

$$d[BR]/dt = [B][R]\,b_{br} - [BR]\,ub_{br}. \tag{29}$$

Suppose the volume of the cell is V. The number of B, BA and BR in the cell are $[\mathrm{B}]V$, $[\mathrm{BA}]V$ and $[\mathrm{BR}]V$. As the total number of B, BA and BR is one, we eliminate B from the above two equations and get

$$d[BA]/dt = (1/V - [BA] - [BR])\,[A]\,b_{ba} - [BT]\,ub_{ba}; \tag{30}$$

$$d[BR]/dt = (1/V - [BR] - [BA])\,[R]\,b_{br} - [BT]\,ub_{br}. \tag{31}$$

Let Pr_{ba} and Pr_{br} be the probabilities of A bound to B and R bound to B. We can write Eq. (30) and (31) in the form of probabilities:

$$d\,\mathrm{Pr}_{ba}/dt = (1 - \mathrm{Pr}_{ba} - \mathrm{Pr}_{br})\,[A]\,b_{ba} - \mathrm{Pr}_{ba}\,ub_{ba}; \tag{32}$$

$$d\,\mathrm{Pr}_{br}/dt = (1 - \mathrm{Pr}_{ba} - \mathrm{Pr}_{br})\,[R]\,b_{br} - \mathrm{Pr}_{br}\,ub_{br}. \tag{33}$$

Assume if a PDP1 is bound to a V/P box, transcription of *clk* gene occurs at a rate of tc_{pc}; if a VRI is bound to the V/P box, transcription rate is tc_{vc} and if nether PDP1 nor VRI binds the V/P box, transcription occurs at a deactivated rate tc_{dvpmt}. The transcription rate of *clk* gene would then be

$$tc_{pc}\,\mathrm{Pr}_{ba} + tc_{vc}\,\mathrm{Pr}_{br} + tc_{dvpmt}\,(1 - \mathrm{Pr}_{ba} - \mathrm{Pr}_{br}). \tag{34}$$

Tables and figures

Table 1 Parameters of the model: The units of binding rates and association rates are $nM^{-1}h^{-1}$ and the units of the other parameters are h^{-1}.

Parameter	Index	Value	Biochemical significance
bccpdpp	1	0.062	binding rate of CLK/CYC to an E-box in *pdp1* promoter
bccperp	2	0.069	binding rate of CLK/CYC to an E-box in *per* promoter
bcctimp	3	0.069	binding rate of CLK/CYC to an E-box in *tim* promoter
bccvrip	4	0.1	binding rate of CLK/CYC to an E-box in *vri* promoter
bpdpclkp	5	1.155	binding rate of PDP1 to a V/P box in *clk* promoter
bvriclkp	6	1.858	binding rate of VRI to a V/P box in *clk* promoter
ubccpdpp	7	0.145	unbinding rate of CLK/CYC to an E-box in *pdp1* promoter
ubccperp	8	0.262	unbinding rate of CLK/CYC to an E-box in *per* promoter
ubcctimp	9	0.262	unbinding rate of CLK/CYC to an E-box in *tim* promoter
ubccvrip	10	0.276	unbinding rate of CLK/CYC to an E-box in *vri* promoter
ubpdpclkp	11	0.952	unbinding rate of PDP1 to a V/P box in *clk* promoter
ubvriclkp	12	1.043	unbinding rate of VRI to a V/P box in *clk* promoter
bcc	13	2.349	association rate of CLK/CYC dimer
bpt	14	1.1	association rate of PER/TIM dimer
bccpt	15	51	association rate of CLK/CYC/PER/TIM complex
ubcc	16	0.89	dissociation rate of CLK/CYC dimer
ubpt	17	2.93	dissociation rate of PER/TIM dimer
ubccpt	18	7.89	dissociation rate of CLK/CYC/PER/TIM complex
tcccpdpp	19	9.831	transcription rate of CLK/CYC-activated *pdp1* gene
tcccperp	20	11	transcription rate of CLK/CYC-activated *per* gene
tccctimp	21	11	transcription rate of CLK/CYC-activated *tim* gene
tcccvrip	22	16.86	transcription rate of CLK/CYC-activated *vri* gene
tcpdpclkp	23	125.54	transcription rate of PDP1-activated *clk* gene
tcvriclkp	24	0.028	transcription rate of VRI-repressed *clk* gene
tcclkp	25	1.42	transcription rate of *clk* gene binding neither PDP1 nor VRI
tcdvpmt	26	0.053	transcription rate of deactivated *per*, *tim*, *vri* or *pdp1* gene
tlclk	27	35	translation rate of *clk* mRNA
tlpdp	28	1.87	translation rate of *pdp1* mRNA
tlper	29	36	translation rate of *per* mRNA
tltim	30	36	translation rate of *tim* mRNA
tlvri	31	14.68	translation rate of *vri* mRNA

dclkm	32	0.643	degradation rate of *clk* mRNA
dpdpm	33	0.06	degradation rate of *pdp1* mRNA
dperm	34	0.053	degradation rate of *per* mRNA
dtimm	35	0.053	degradation rate of *tim* mRNA
dvrim	36	0.07	degradation rate of *vri* mRNA
dclk	37	0.2	degradation rate of CLK protein
dpdp	38	0.156	degradation rate of PDP1 protein
dper	39	0.62	degradation rate of PER protein
dtim	40	0.62	degradation rate of TIM protein
dvri	41	1.226	degradation rate of VRI protein
dpt	42	0.279	degradation rate of PER/TIM dimer
dcc	43	0.184	degradation rate of CLK/CYC dimer
dccpt	44	15.122	degradation rate of CLK/CYC/PER/TIM complex
npt	45	5	number of E-boxes in *per* or *tim* promoter
nvri	46	4	number of E-boxes in *vri* promoter
npdp	47	6	number of E-boxes in *pdp1* promoter

Table 2 Initial conditions. Abbreviations: CC – CLK/CYC, PT – PER/TIM, CCPT – CLK/CYC/PER/TIM. Constant values in the system are remarked by *.

Specie	Concentration (nM)	Specie	Concentration (nM)
CC	0.5566	clkp*	0.003185
CCPT	0.4982	pdpp*	0.003185
CLK	3.6628	perp*	0.003185
clkm	0.2583	timp*	0.003185
PDP	4.1953	vrip*	0.003185
pdpm	0.3175		
PER	2.7527		
perm	0.2395	Probability	Value
PT	0.4014	prcpdp	0.08
TIM	2.7527	prcper	0.0431
timm	0.2395	prct	0.043
VRI	3.175	prcv	0.0585
vrim	0.2571	prpc	0.426
CYC*	100.0	prvc	0.489

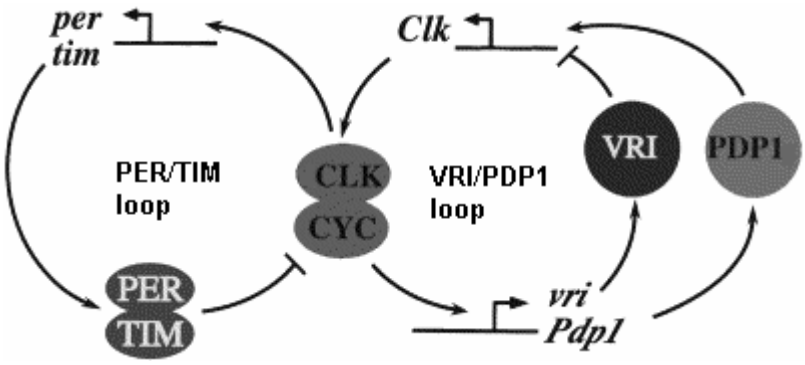

Figure 1 Two interacted loop model (Adapted from Cryan, 2003): In summary, circadian rhythms are generated by the action of two interacting feedback loops, named the PER/TIM loop and the VRI/PDP1 loop. In the first loop, rhythmic transcription of the *per* and *tim* genes is controlled by feedback from their own protein products, which form PER/TIM dimers and inhibit the activity of their positive transcription factors CLK/CYC dimers. In the second loop, transcription of *vri* and *Pdp1* genes is activated by CLK/CYC, and their products VRI and PDP1 activate and repress *clk* gene respectively. The two feedback loops are linked together by requirement of CLK/CYC dependent transcription and start simultaneously.

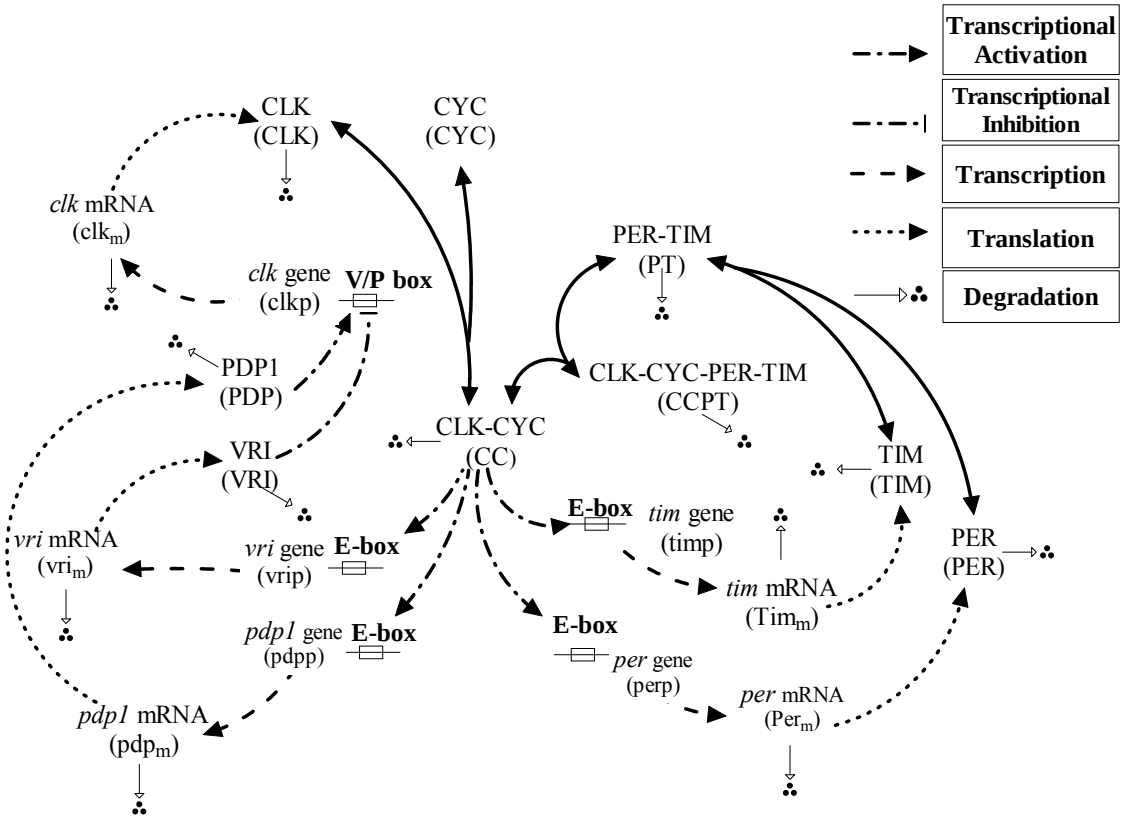

Figure 2 The schematic diagram of the model. The model shows the regulatory relationships among genes, mRNAs and proteins in the negative and positive transcriptional feedback loops. Transcription of *per*, *tim*, *vri* and *pdp1* genes are activated by CLK/CYC dimers binding to E-boxes in their promoter regions. In one loop, *per* and *tim* mRNAs are translated to PER and TIM proteins which form PER/TIM dimers. PER/TIM binds to CLK/CYC to form PER/TIM/CLK/CYC complex. In another loop, *vri* and *pdp1* mRNAs are translated to VRI and PDP1 proteins. They compete to bind a V/P box in the promoter in *clk* gene. Transcription of *clk* gene is repressed by VRI and activated by PDP1. *clk* mRNA is translated to CLK which forms CLK/CYC dimer with CYC. Proteins, mRNAs, dimers and complexes are degraded at certain kinetic rates. CYC is assumed to be constant therefore there is no degradation of CYC. Variable names used in the model are indicated in the parentheses. The number of E-boxes in the promoters is not shown here.

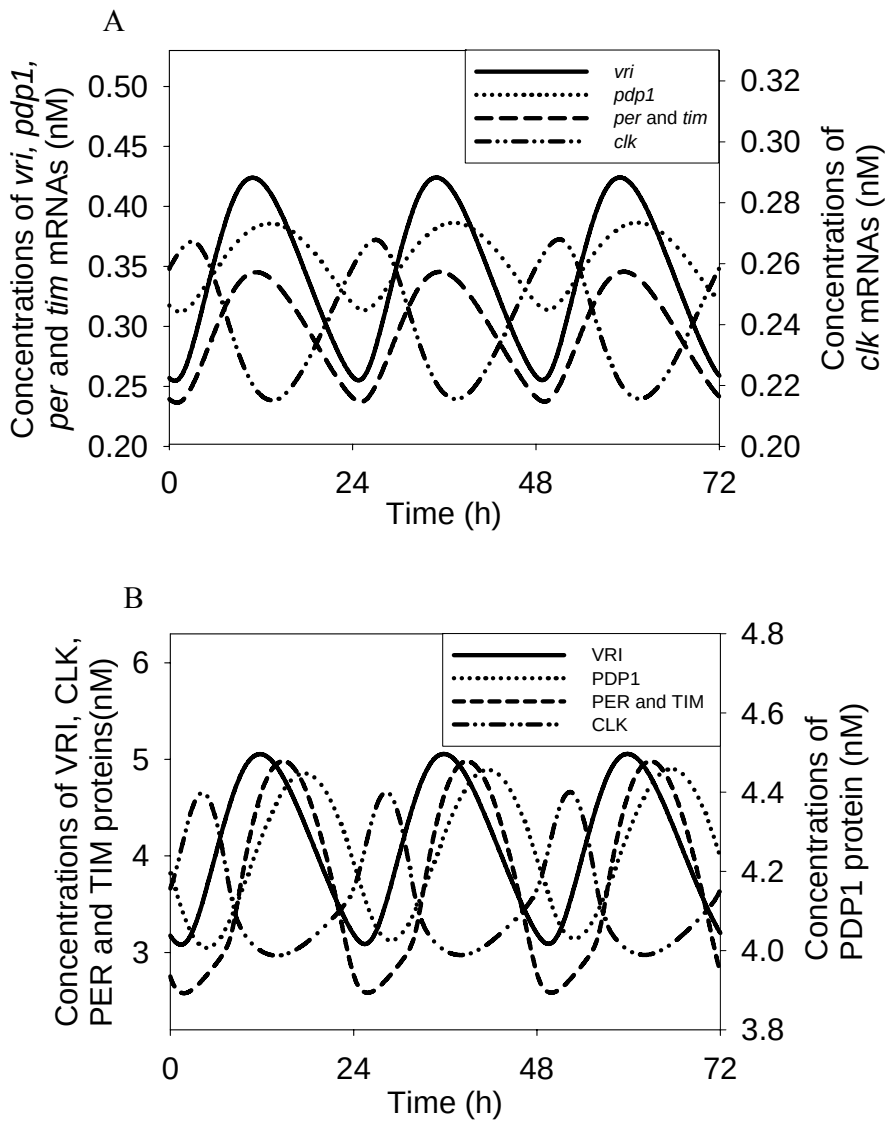

Figure 3 Sustained oscillations for the concentrations of the mRNAs and the proteins: (A) Oscillations for the mRNAs and (B) oscillations for the proteins. The Time scale of *clk* in (A) and PDP1 in (B) has been enlarged for better visualisation.

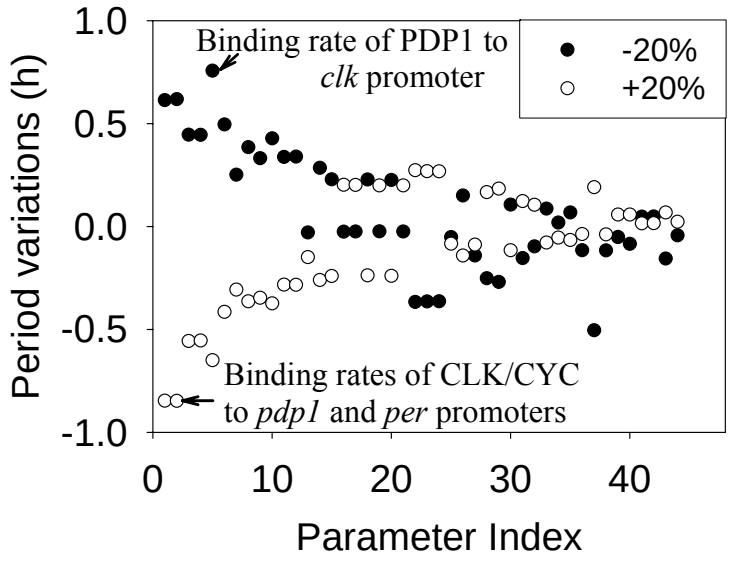

Figure 4 Period variations of the circadian oscillations in respect of parameter variations, one parameter was increased or decreased by 20% once while the other parameters were kept at the basal values. The most sensitive parameters are indicated. Parameter names corresponding to the parameter index are denoted in Table 1.

A

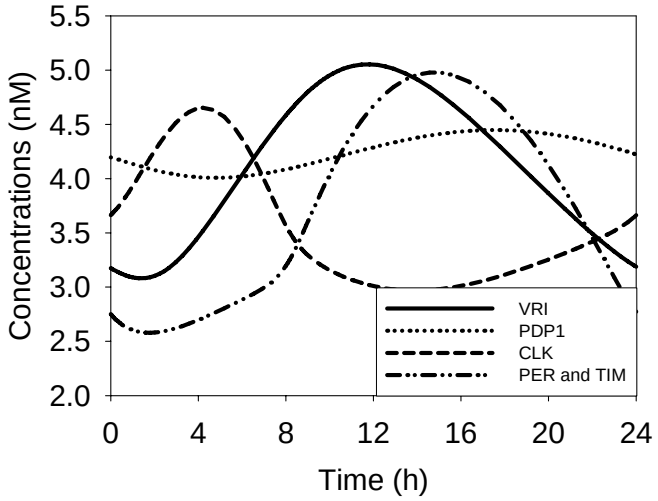
Concentrations (nM)
5.5
5.0
4.5
4.0
3.5
3.0
2.5
2.0
0
4
8
12
16
20
24
Time (h)
VRI
PDP1
CLK
PER and TIM

B

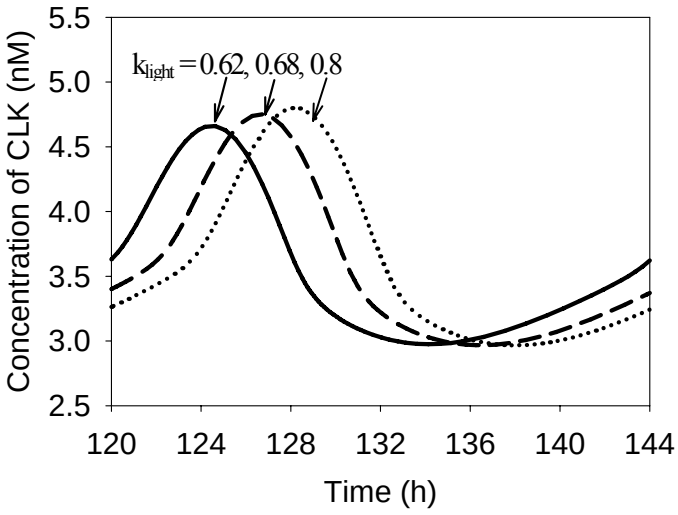
Concentration of CLK (nM)
5.5
5.0
4.5
4.0
3.5
3.0
2.5
k_{light} = 0.62, 0.68, 0.8
120
124
128
132
136
140
144
Time (h)

C

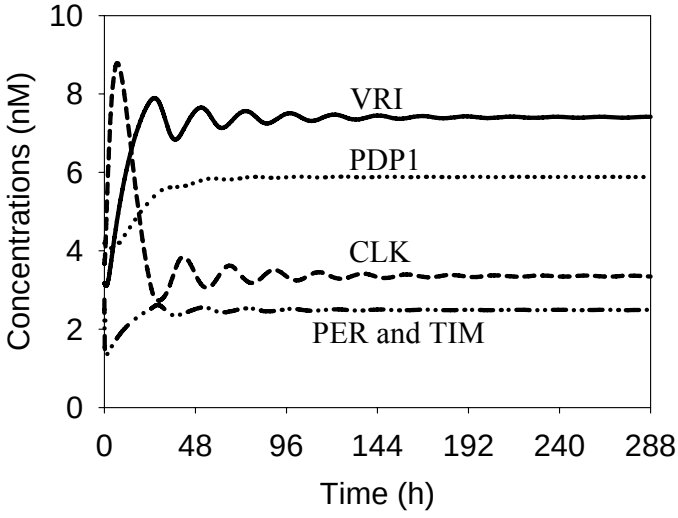
Concentrations (nM)
10
8
6
4
2
0
0
48
96
144
192
240
288
Time (h)
VRI
PDP1
CLK
PER and TIM

Figure 5 (A). Entrainment by LD cycle. k_{light} is increased (0.8) during the light phase and remains at the original value (0.62) during the dark phase. Simulation was done with ZT0 lights on, ZT12 lights off. (B). The phases of oscillations after entrainment depend on the different values of k_{light}. We plotted the 6^{th} cycle after the cycles were stable to eliminate the transient effect of light. (C). Rhythmicity disappears in constant light condition when $k_{light} > 5$. A k_{light} value of 5 was used to produce this figure.

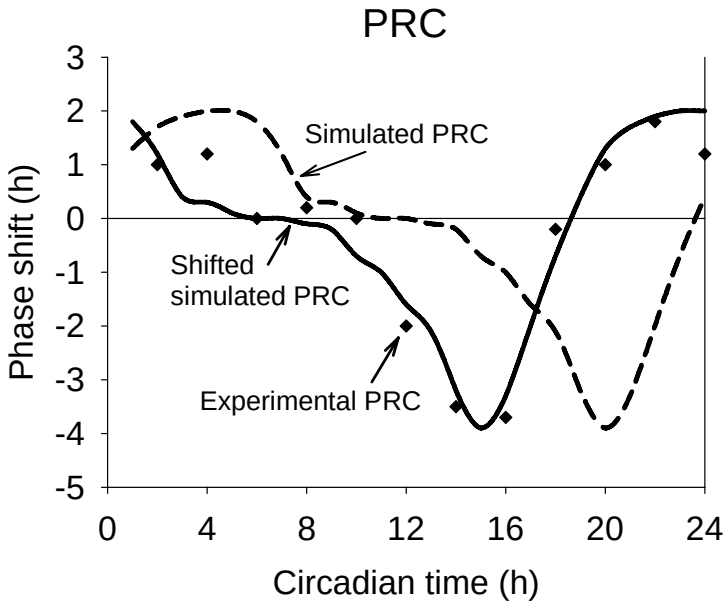

Figure 6 Phase response curve (PRC) obtained by using k_{light} = 1.3. The x-axis represents the time of onset of each light pulse, and on the y-axis positive values represent phase advance and the negative values represent phase delays. The means of experimental values for phase shifts from Konopka (1991) are denoted by diamonds. The simulated PRC is shown by the dashed curve and the shifted simulated PRC is shown by the solid curve. The shifted simulated PRC was obtained by advancing the simulated PRC by 5 h, and it is plotted here only for comparison purpose.

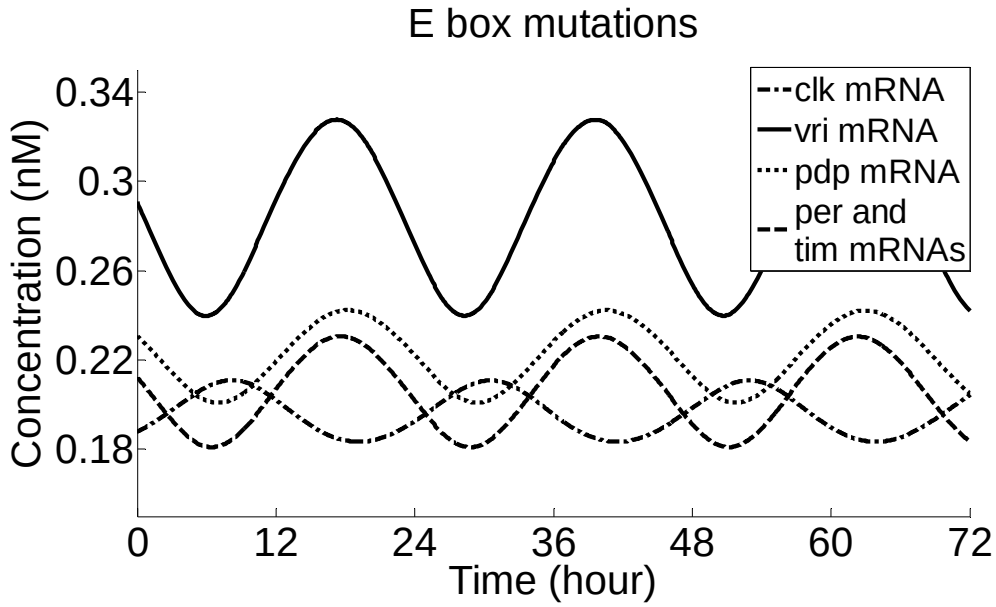

Figure 7 mRNA oscillations in E-boxes mutation simulation, where only one copy of E-box remains in each type of gene.

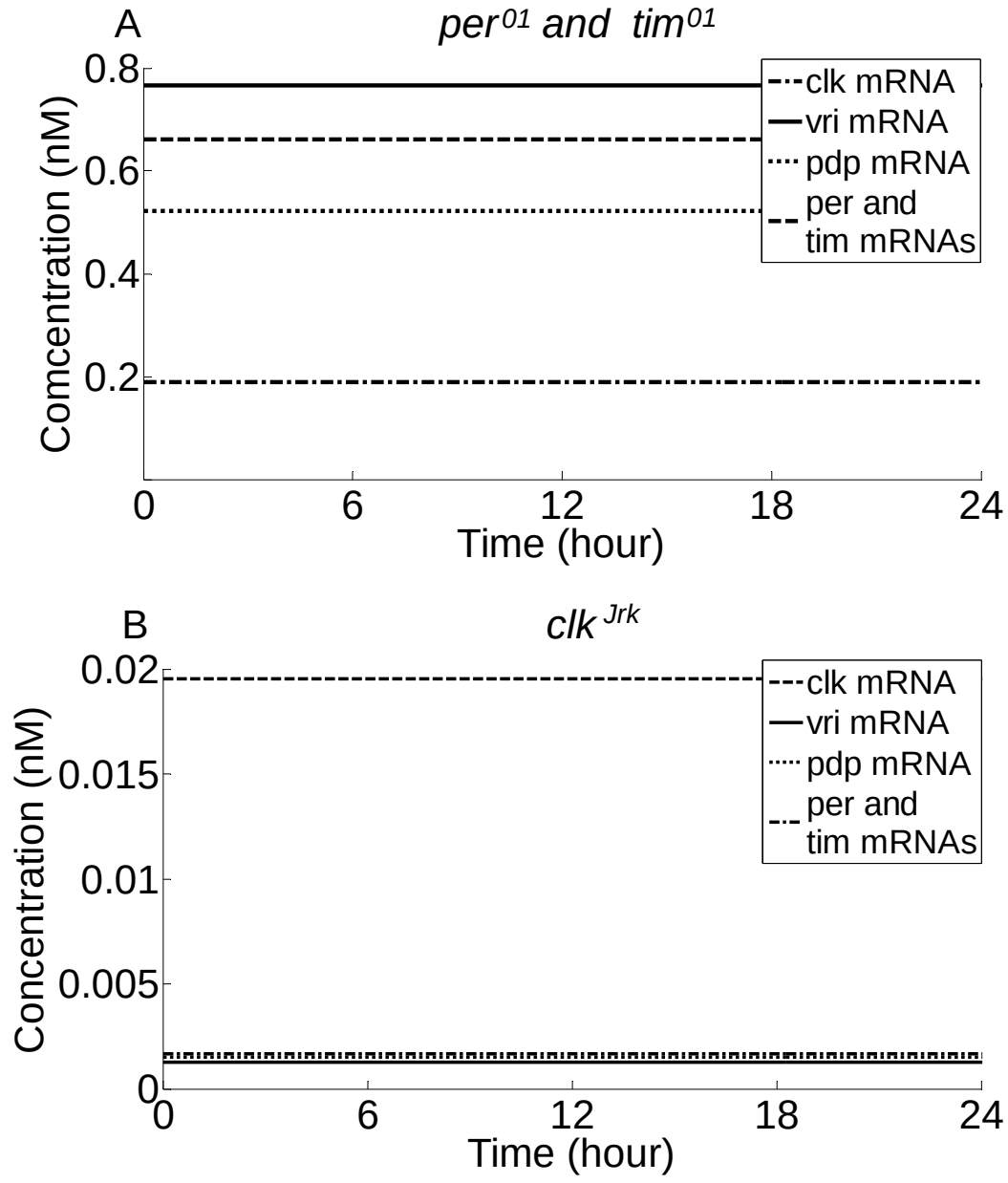

Figure 8 Simulation of arrhythmic mutants. Parameter values are as in Table 1, expect for tlper=0 for *per*^{01}, tltim=0 for *tim*^{01} and tlclk=0 for *clk*^{Jrk}.

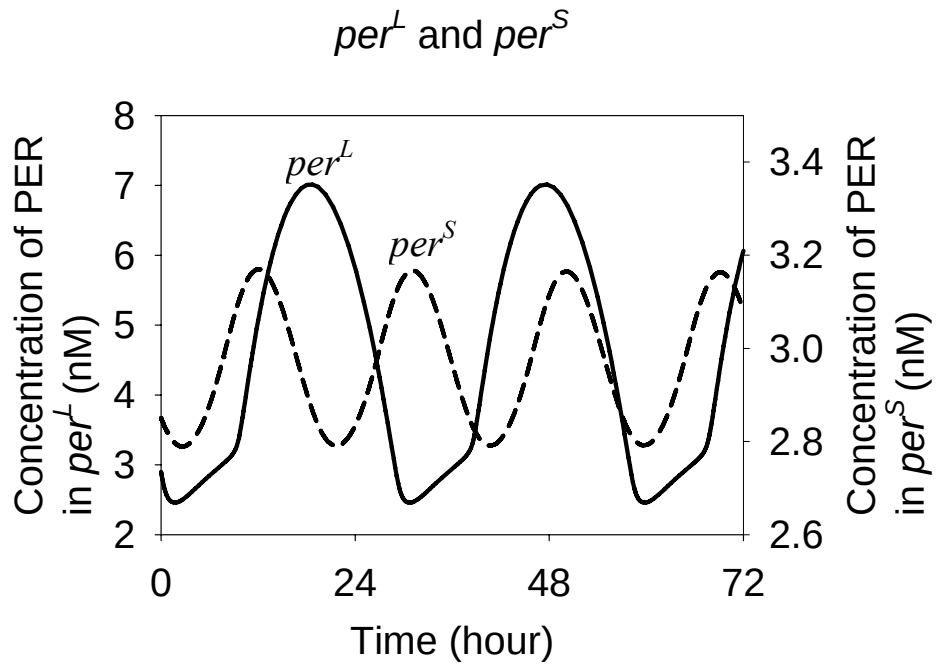

Figure 9 Simulation of short and long mutants. Parameters values are as in Table 1, expect for dpt=0.9 for *per*^{S} and dpt=0.08 for *per*^{L}.